Mutual Information Effective SNR Mapping Algorithm for Fast Link Adaptation Model in 802.16e

Fernando López Aguilar, Gorka Rubio Cidre, José Manuel López López, and Javier Regidor Paris

Telefónica I+D
Emilio Vargas, 6, 28043 Madrid, Spain
{fla,gorka,josemll,javirp}@tid.es

Abstract. The Always Best Connected Systems (ABCS) philosophy, in which different access technologies coexist, allows the user to select at any time an appropriate network that is optimized for the current service. To study this scenario through simulations, it is needed that all simulators are system-level type. Regarding this point, Effective SNR Mapping (ESM) algorithms provide the link layer abstraction that is crucial for the system level simulation interface. In this paper we have used the Mutual Information Effective SNR Mapping (MIESM) algorithm for instantaneous-channel modelling, calibration and evaluation of the Link Level Interface in the WiMAX System 802.16e together with a realistic Mobile WiMAX simulator. Plenty of simulations were performed to evaluate different algorithms and the results show that MIESM gives higher accuracy than the rest of ESM methods.

Keywords: Link layer abstraction, effective *SNR*, MIESM, 802.16e, Mobile WiMAX, H-ARQ, AMC and PUSC/FUSC.

1 Introduction

In OFDM (Orthogonal Frequency Division Multiplexing) Multi-Carrier simulators, the system level usually interfaces with the link level using SNR (Signal to Noise Ratio) Mapping methods. As a result, complexity is reduced and performance benefits from shorter simulation times. Mapping methods surpass classical methods from the calibration point of view, characterizing each Modulation and Coding Scheme (MCS) in multipath channels taking into account shadowing, Doppler Effect, reception diversity and other effects that deteriorate the transmission.

Although most works in literature deal with OFDM aspects, our work aims at realistic simulations of 802.16e. Special aspects such as H-ARQ (Hybrid Automatic Repeat Request), Partial Use of Sub-Carriers (PUSC)/Full Use of Sub-Carriers (FUSC) permutations and AMC (Adaptive Modulation and Coding) play an important part in our simulations. As for the calibration phase, the MIESM (Mutual Information Effective SNR Mapping algorithm) is used. The ultimate goal is to reach calibration results that accurately match real situations.

P. Chatzimisios et al. (Eds.): MobiLight 2010, LNICST 45, pp. 356–367, 2010.

The link-to-system mapping look-up table is built following the procedure shown in Fig. 1 [3]. For each MCS, simulations are performed over a wide range of effective SNR to estimate the block error rate, the calibration factor (β) and the mean square error.

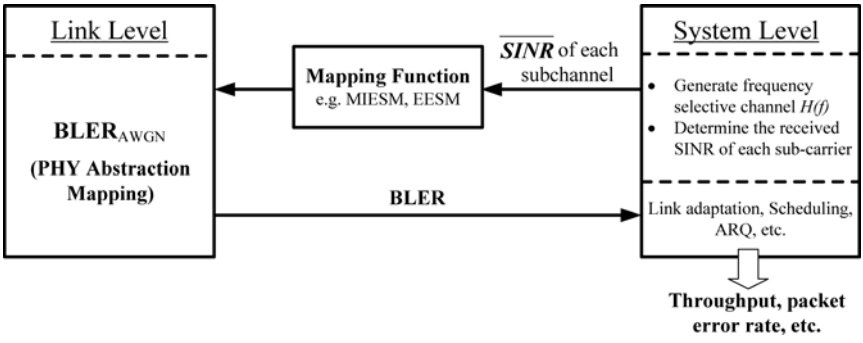

Fig. 1. Link-to-system mapping procedure

The rest of the paper is organized as follows. Section 2 describes the link level simulator. Section 3 reviews the Mutual Information Effective SNR Mapping algorithm to be used in conjunction with the simulator. The simulation parameters and results are presented and analyzed in Section 4. Finally, section 5 summarizes the conclusions and foresees future work on the subject.

2 Description of the Mobile WiMAX Link Level Simulator

The Mobile WiMAX Simulator, whose architecture is shown in Fig. 2, is a standalone application compiled in Visual C++ for Windows, that seeks to emulate a single link (the first two layers, physical and MAC –Media Access Control–) of this broadband wireless solution (IEEE 802.16e), that will play a key role in metropolitan area networks, enabling the convergence of mobile and fixed broadband radio access technologies and flexible network architecture. Mobile WiMAX systems offer scalability in both radio access technology and network architecture, thus providing a great deal of flexibility in network deployment options and service offerings.

The IEEE 802.16e Wireless MAN OFDMA mode [9] is based on the concept of scalable OFDMA (S-OFDMA). S-OFDMA supports a wide range of bandwidths to flexibly address the need for various spectrum allocation and usage model requirements. The scalability is supported by adjusting the FFT (Fast Fourier Transform) size while fixing the sub-carrier frequency spacing at 10.94 kHz.

This technology supports sub-channelization in both Down Link (DL) and Uplink (UL), and there are two types of sub-carrier permutations for sub-channelization: diversity-based and contiguous. The diversity permutation draws sub-carriers pseudo-randomly to form a sub-channel. It provides frequency diversity and inter-cell interference averaging. The diversity permutations include DL FUSC (Fully Used Sub-Carrier), DL PUSC (Partially Used Sub-Carrier), UL PUSC and additional optional permutations

such as Adaptive Modulation and Coding (AMC). With DL PUSC, for each pair of OFDM symbols, the available or usable *sub-carriers* are grouped into *clusters* containing 14 contiguous sub-carriers per symbol period, with *pilot* and *data* allocations in each cluster in the even and odd symbols. The available sub carrier space is split into *tiles* and six *tiles*, chosen from across the entire spectrum by means of a re-arranging/ permutation scheme, and grouped together to form a *slot*. The *slot* comprises 48 data sub-carriers and 24 pilot *sub-carriers* in 3 OFDM symbols. The contiguous permutation groups a block of contiguous *sub-carriers* to form a *subchannel*. The contiguous permutations include DL AMC and UL AMC, and have the same structure. A *bin* consists of 9 contiguous *sub-carriers* in a *symbol*, with 8 assigned for *data* and one assigned for a *pilot*. A *slot* in AMC is defined as a collection of *bins* of the type (N x M = 6), where N is the number of contiguous *bins* and M is the number of contiguous *symbols*. Thus the allowed combinations are [(6 *bins*, 1 *symbol*), (3 *bins*, 2 *symbols*), (2 *bins*, 3 *symbols*), (1 *bin*, 6 *symbols*)]. AMC permutation enables multi-user diversity by choosing the sub-channel with the best frequency response.

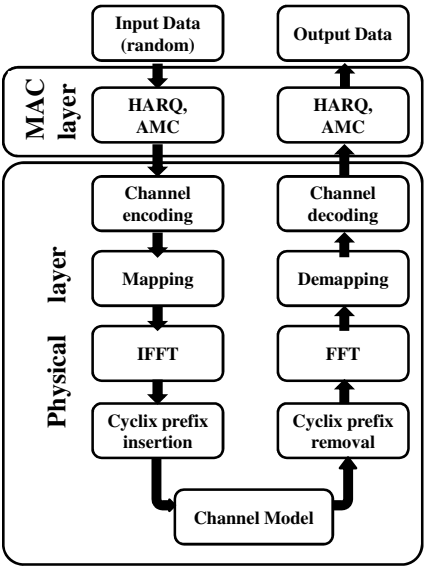

Fig. 2. Architecture of Mobile WiMAX Simulator

In general, diversity *sub-carrier* permutations perform well in mobile applications while contiguous *sub-carrier* permutations are well suited for fixed, portable, or low mobility environments. These options enable the system designer to trade-off mobility for throughput.

H-ARQ is supported by Mobile WiMAX. H-ARQ is enabled using an N channel "Stop and Wait" protocol which provides fast response to packet errors and improves cell-edge coverage. Chase Combining and optionally Incremental Redundancy are supported to further improve the reliability of the retransmission. A dedicated ACK channel is also provided in the uplink for H-ARQ ACK/NACK signalling. Multi-channel

H-ARQ operation is also supported. Multi-channel stop-and-wait ARQ with a small number of channels is an efficient, simple protocol that minimizes the memory required for H-ARQ and stalling. WiMAX provides signalling to allow fully asynchronous operation. The asynchronous operation allows variable delay between retransmissions which gives more flexibility to the scheduler at the cost of additional overhead for each retransmission allocation. H-ARQ, combined together with CQICH (Channel Quality Indicator CHannel) and AMC, provides robust link adaptation in mobile environments at vehicular speeds in excess of 120 km/h.

Rayleigh fading is the statistical model used in this simulator, which emulates the effect of shadowing, multipath, Doppler and cross polarization discrimination (XPD), also taking into account advanced techniques such as diversity reception and antenna correlation. All these parameters, together with mobile terminal speed, are fixed initially in the simulator before starting the simulation.

Finally, we use a frequency selective wireless channel that can be modelled by a tapped delay line channel model (time-variant Finite Impulse Response –FIR– filter in complex equivalent low-pass signal domain). The number of FIR taps is given by the power delay profile of the channel, or the r.m.s. (root mean square) delay spread of the channel. Both are configured at the beginning of the simulation. Each of the complexes FIR taps changes over time. The time delays between the multipath components depends on both the surrounding reflectors and the antennas involved, imposing a distinction among propagation paths between base stations and propagation paths from a base station to the users. Depending on the antennas used and the transmission environment, multipath components with significant delay spreads will occur. The amplitude (in dB) of each FIR tap has the statistics of a Rayleigh random process, and the way it changes over time is determined by the Doppler spectrum of the channel, where the relative motion between base station and mobile terminal (or surrounding objects causing e.g. reflection) causes random frequency modulation, since each multipath component has a different Doppler shift (phase change per time unit). Known the influence on the system performance of specific antenna characteristics (radiation pattern, polarization characteristics, cross-polarization discrimination) in MIMO (Multiple Input Multiple Output) systems, the radio link takes into account the XPD of the antennas.

3 Review of Mutual Information Effective SNR Mapping Algorithm

The link-to-system mapping methods can be effectively used in OFDM communication systems through using the effective SNR concept [2][10]. Some of these methods are based on Mutual Information metrics. The MIESM algorithm defines the mutual information on the bit channel itself, which we will refer to as the mutual information per coded bit to build the optimized function for each modulation scheme.

A block diagram for the MIESM approaches is shown in Fig. 3. Given a set of N received encoder symbol SINRs (Signal to Interference-plus-Noise Ratios) from the system level simulation, denoted as $SINR_1$, $SINR_2$, $SINR_3$, …, $SINR_N$, a mutual information metric is computed. Based on the computed MI-metric an equivalent SINR is obtained and used to look-up the BLER (BLock Error Rate).

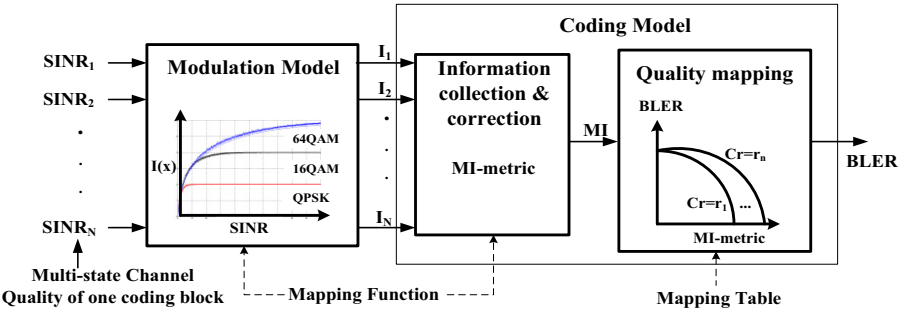

Fig. 3. Effective mapping abstraction procedure

The computation of MIESM is based on the nonlinear mapping relationship from *SINR* to mutual information to calculate the effective *SINR*, as we can see in equation (1)[2], in which β is a calibration factor whose value is chosen to minimize the root mean square (r.m.s) error between the effective SNR, derived from the Rayleigh channel, and the static SNR which leads to the same BLER value:

$$SNR_{eff} = \beta \cdot I^{-1}\left(\frac{1}{P}\sum_{p=1}^{P} I\left(\frac{SINR_p}{\beta}\right)\right) \tag{1}$$

Here, I is the mutual information function, taking into account the modulation type. The obtaining of I is based on equation (2), in which m_p is the bits per symbol, X is the set of symbols, X_b^i is the set of symbols for which bit i equals b. Y is a zero mean unit variance complex Gaussian random variable.

$$I_{m_p} = m_p - E_y\left\{\frac{1}{2^{m_p}}\sum_{i=1}^{m_p}\sum_{b=0}^{1}\sum_{z\in X_b^i} log_2 \frac{\sum_{\hat{x}\in X} e^{-\left|Y-\sqrt{x}(\hat{x}-z)^2\right|}}{\sum_{\tilde{x}\in X} e^{-\left|Y-\sqrt{x}(\tilde{x}-z)^2\right|}}\right\} \tag{2}$$

This equation provides the curves shown in Fig. 4. Hence the constellation points of 16-QAM and 64-QAM are normalized by a factor to ensure that the average energy over all symbols is one. Curves are compared against the IEEE reference model [3].

Detailed below are the needed steps to obtain the SNR_{eff} and the optimal β based on the equation (1) and (2):

Step 1. Obtain the BLER vs. SNR curve for an Additive White Gaussian Noise (AWGN) channel.

Step 2. Obtain a high number of BLER vs. SNR curves for a tapped delay Rayleigh channel (3GPP Extended Pedestrian A –EPA– channel model) performing simulations. Gather SNR per subcarrier data as part of the simulations.

Step 3. Find the BLER values obtained in Step 2 (Rayleigh) into the AWGN curve. We called this $SNR_{statics}$ where S is the number of simulated points (Number of curves for EPA channel model multiplied by the number of points of each curve).

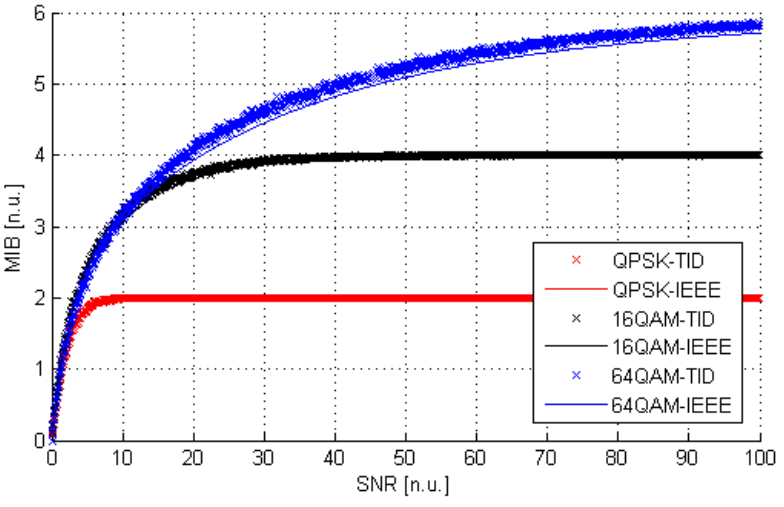

Fig. 4. MIB vs. SNR, both calculated by us and modelled by IEEE

Step 4. For each SNR_{static_S} value, we know the associated value of BLER, SNR evaluated and the SNR per subcarrier ($SINR_P$). The SNR per subcarrier will be translated into a SNR effective (SNR_{eff_S}, where S is the number of simulated points) with the appropriate equation for MIESM algorithm described below. This SNR_{eff} is a function which depends on β and I. The key formula used has been shown in (1).

Step 5. Finally, we iterate for a large range of β values to obtain the optimal β through the minimization of the root mean square error (r.m.s) between SNR_{eff_S} and SNR_{static_S}. This is calculated using equations (3) and (4):

$$r.m.s. = \frac{1}{S}\sum_{s=1}^{S}\left(SNR_{eff_s} - SNR_{static_s}\right)^2 \tag{3}$$

$$\beta = \arg min(r.m.s.) \tag{4}$$

4 Simulation Results

In this section, we verify the abstraction algorithm performance. The multipath channel mode considered is EPA, as is specified in [7], at pedestrian speed (3 km/h). The tapped delay line model used in our Rayleigh simulations is shown in Fig. 5.

The simulation was performed in the frequency domain using 360 data sub-carriers spaced 10.94 KHz. For each channel realization there are 2000 simulated frames. The PUSC permutation schemes [8] have the advantages of distributed subcarrier allocation and are well suited for mobile, fast-moving subscribers. Incremental-Redundancy- based H-ARQ is selected taking the puncture pattern into account, and for each retransmission the coded block is not the same. We also use H-ARQ due to the fact that it provides a

significant advantage throughout the range of practically relevant SNRs. In addition, incremental redundancy is selected because it is shown to outperform lower-complexity Chase combining, particularly at moderate and high SNRs. The whole configuration parameters of the simulation can be seen in Table 1.

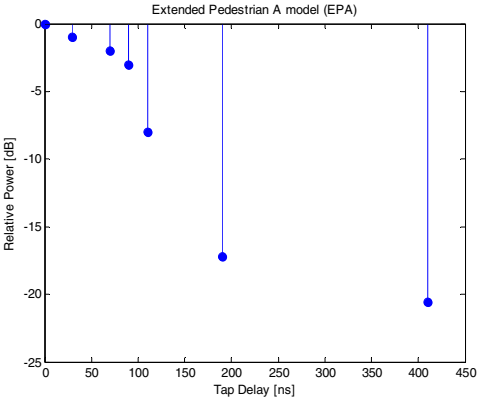

Fig. 5. 3GPP Extended Pedestrian A model EPA (Tapped Delay Channel) Multi-Path Environments with Classic Doppler Spectrum.

Table 1. Link Level Simulator Parameters

Parameter	Value
Carrier Frequency	3.5GHz
Bandwidth	5MHz
Sub-Carrier Spacing	10.94KHz
Sampling Frequency	5.6 MHz
FFT Size	512
Number of Sub-Channels	8
Useful Symbol Time	91.4 µs
Guard Time	11.4 µs
OFDMA Symbol Duration	102.9 µs
Null Sub-Carriers	92
Pilot Sub-Carriers	60
Data Sub-Carriers	360
Sub-Channels	15

Parameter	Value
Symbol Period, Ts	102.9µs
Frame Duration	5ms
OFDM Symbols/Frame	48
Data OFDM Symbols	44
Permutation	PUSC
Simulated Frames	2000
XPD	10 dB
Channel Estimation	Real (Pilots)
H-ARQ	Incremental Redundancy
Power Delay Profile	AWGN and EPA channel model, Extended Typical Urban (ETU) [7]
Mobile speed	Pedestrian (3Km/h)
Antenna Scheme	SIMO Correlated Antennas. Diversity Reception (10dB)

The different Modulation Coding Schemes (MCS) used are defined based on Modulation, Coding Rate using Turbo Code Codification and Repetition Factor[9]. The possible options are shown in Table 2.

Table 2. Transmission mode parameters

Modulation	Coding Rate	Repetition Factor	Modulation Coding Scheme
QPSK	½ CTC	x6	MCS1
	½ CTC	x4	MCS2
	½ CTC	x2	MCS3
	½ CTC	x1	MCS4
	¾ CTC	x1	MCS5
16QAM	½ CTC	x1	MCS6
	¾ CTC	x1	MCS7
64QAM	½ CTC	x1	MCS8
	2/3 CTC	x1	MCS9
	¾ CTC	x1	MCS10
	5/6 CTC	x1	MCS11

Fig. 6 shows the result of the execution of Step 1 (reference curves for all MCS) as we explained in Section 3. The different modes are shown in ascendant order based on Table 2 with a spatial separation of approximately 2dB. Red lines correspond to QPSK modulation, green lines correspond to 16QAM and blue lines correspond to 64QAM.

Although Fig. 7 is not necessary to calculate β, we show it in order to validate our whole simulation process. The Downlink Rate obtained is almost the same as the theoretical values [9].

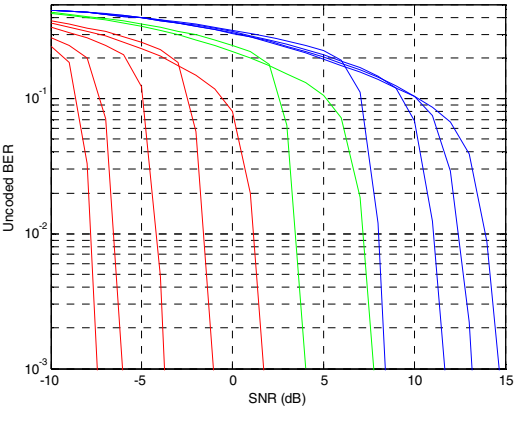

Fig. 6. Uncoded BER vs. SNR for different transmission modes in AWGN channel @ 3km/h

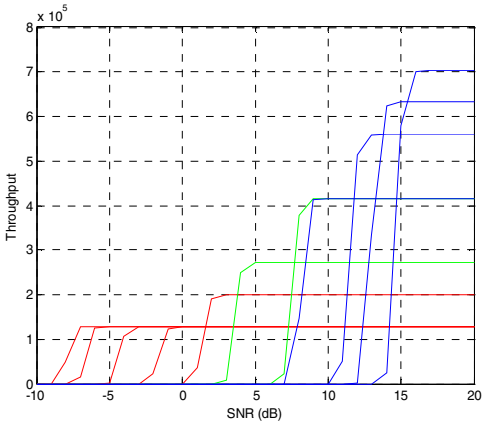

Fig. 7. Link level throughput with HARQ in AWGN channel @ 3km/h

Table 3 shows β and r.m.s error values obtained for the MIESM algorithm evaluated in this paper and the ESM methods described in [1]. These values are obtained using the formulas described in Section 3.

Table 3. β and r.m.s. error values for different MCSs in MIESM

MCS	β_{MIESM}	error	β_{EESM}	error	β_{CESM}	error	β_{LESM}	error
1	1.03	0.010	1.68	0.055	0.08	0.165	-0.29	0.090
2	1.07	0.015	1.71	0.017	0.09	0.121	-0.24	0.015
3	1.11	0.019	1.73	0.023	0.12	0.228	-0.22	0.020
4	1.15	0.021	1.75	0.121	0.16	0.218	-0.19	0.117
5	1.18	0.028	1.78	0.055	0.19	0.153	-0.17	0.056
6	1.09	0.026	5.29	0.088	0.23	0.183	-0.16	0.090
7	1.13	0.018	7.51	0.102	0.03	0.188	0.27	0.175
8	1.06	0.017	12.57	0.087	0.05	0.291	0.29	0.079
9	1.12	0.011	16.21	0.120	0.09	0.225	0.35	0.122
10	1.16	0.013	27.27	0.139	0.12	0.370	0.39	0.169
11	1.17	0.014	32.14	0.178	0.15	1.180	0.44	0.196

It is noticeable that r.m.s error and β values do not increase if MCS modes go higher. Comparing MIESM to other ESM algorithms (EESM, CESM and LESM) from [1], we can draw the conclusion that MIESM gives better accuracy (in terms of r.m.s. error) than the others.

Fig. 8 and Fig. 9 show the difference of the BER calibration results from the MIESM algorithm in MCS1 and MCS10, using the configuration parameters shown in

Table 2. The scattered markers are the BER measurements obtained with multipath channel, while the solid line is the reference BER curve for AWGN channel.

The use of an analytical function to calculate the inverse Mutual Information would increase the calibration precision especially in lower modulation schemes where the experimental curves quickly increase towards asymptotic values (see Fig. 4), making difficult the estimation of the inverse Mutual Information needed in (1).

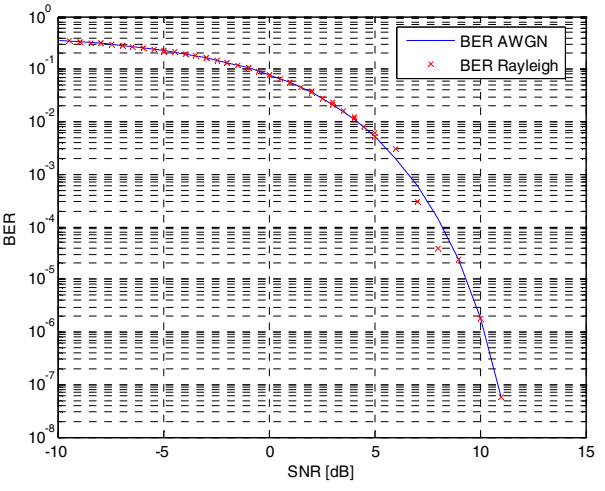

Fig. 8. MIESM Calibration Results for MCS1

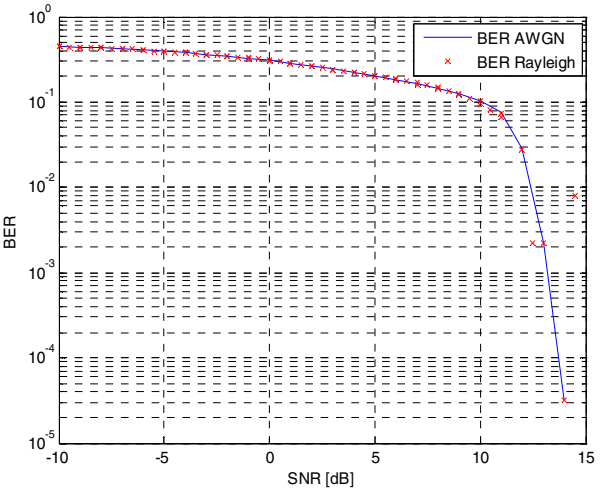

Fig. 9. MIESM Calibration Results for MCS10

5 Conclusions and Future Work

In this paper, the Mutual Information Effective SNR Mapping (MIESM) method for link-to-system mapping has been used in conjunction with an 802.16e link level simulator as a building block for a complete system level simulator. Simulations take into account the singularities of the 802.16e physical layer and important features of the MAC layer as well, such as H-ARQ, PUSC/FUSC and AMC. The results show that MIESM outperforms the other methods studied by us in [1]. The resulting calibration factor (β) brings the effective SNR curve closer to the reference AWGN curve, hence resulting in higher accuracy (lower r.m.s. error) than other methods. This holds especially for higher modulation schemes (large number of symbols). It is explained easily with the use of the equation described in (2).

Future work will continue studying realistic simulations using promising methods for link-to-system mapping such as weighted-training MIESM and Mean Mutual Information per Bit (MMIB) ESM. The use of an analytical function to calculate the inverse Mutual Information will also increase the calibration precision.

Acknowledgments. This research has been partially supported by the CELTIC ICARUS project "Distributed Wireless Networking Experimental Infrastructure for Optimization and Convergence" and funded by the Ministerio de Industria, Turismo y Comercio (TSI-020400-2008-113) of Spain.

We would like to thank Javier Lorca from the Radio Communication Group at Telefónica I+D for his support on the simulator used for this paper.

References

1. Aguilar, F.L., Cidre, G.R., López, J.M.L., París, J.R.: Effective SNR Mapping Algorithms for Link Prediction Model in 802.16e. In: International Conference on Ultra Modern Telecommunications & Workshops ICUMT 2009, pp. 1–6. IEEE, Los Alamitos (2009)
2. He, X., Niu, K., He, Z., Lin, J.: Link Layer Abstraction in MIMO-OFDM System. In: International Workshop on Cross Layer Design, IWCLD 2007, pp. 41–44. IEEE, Los Alamitos (2007)
3. Zhuang, J., Jalloul, L., Novak, R., Park, J.: IEEE 802.16m Evaluation Methodology Document (EMD). In: Srinivasan, R. (ed.) IEEE 802.16 Broadband Wireless Access Working Group. Intel Corporation (2009)
4. Mumtaz, S., Gameiro, A., Rodríguez, J.: EESM for IEEE 802.16e: WiMax. In: 7th IEEE/ACIS International Conference on Computer and Information Science, IEEE, Los Alamitos (2008)
5. Toumaala, E., Wang, H.: Effective SINR Approach of Link to System Mapping in OFDM/Multi-Carrier Mobile Network. In: 2nd International Conference on Mobile Technology, Applications and Systems, pp. 1–5. IEEE, Los Alamitos (2005)
6. Olmos, J., Serra, A., Ruiz, S., García-Lozano, M., Gonzalez, D.: Exponential Effective SIR Link Performance Model for LTE Downlink. European Cooperation in the Field of Scientific and Technical Research. Technical report, EURO-COST (2009)

7. 3GPP TS 36.104, Evolved Universal Terrestrial Radio Access (E-UTRA); Base Station (BS) Radio Transmission and Reception (Release 8), v8.4.0. Technical specification, 3GPP (2008)
8. Bykovnikov, V.: The Advantages of SOFDMA for WiMAX. Technical report. Intel Corporation (2005)
9. Part 16: Air Interface for Fixed and Mobile Broadband Wireless Access Systems. Amendment 2: Physical and Medium Access Control Layers for Combined Fixed and Mobile Operation in Licensed Bands. IEEE Std. 802.16e-2005, IEEE (2005)
10. Guidelines for evaluation of radio interface technologies for IMT-Advanced, ITU-R M.2135, ITU (2008)